Materials
Views
www.MaterialsViews.com

ADVANCED
MATERIALS
www.advmat.de

COMMUNICATION

Biologically Inspired Omniphobic Surfaces by Reverse Imprint Lithography

René Hensel, Andreas Finn,Ralf Helbig, Hans-Georg Braun, Christoph Neinhuis, Wolf-Joachim Fischer, and Carsten Werner*

Motivated by botanical studies,[1,2] lotus-leaf-inspired superhydrophobic surfaces have attracted attention due to their excellent repellence of water droplets and resulting self-cleaning capability.[3,4] Upon immersion into aqueous media, such surfaces effectively retain air that can, for instance, facilitate drag reduction in microfluidic devices[5] or on ship hull coatings.[6] Furthermore, superhydrophobic surfaces can prevent biofouling due to a minimized contact area between the applied medium and the solid surface.[7,8] Accordingly, superhydrophobic leaves have motivated the development of self-cleaning, drag-reducing, or antifouling applications. However, in practice, artificial surfaces that mimic the needle or pillar structures of plants[9] show fundamental limitations: 1) Wetting by low-surface-tension liquids such as oils or water contaminated by detergents, surfactants or soluble substances that decrease the surface tension cannot be prevented.[4] 2) The energetic barrier against complete wetting of the surface is often even less than the kinetic energy of falling rain droplets and, thus, the structures are neither applicable for outdoor coatings nor suitable for large immersion depths.[10,11] 3) The mechanical stability and, in particular, the resistance against shear loads by scratching[12,13] and against collapse due to capillary forces in dense arrays[14,15] are insufficient for nanoscopic needle or pillar structures, which limits the long-term durability of these surfaces. Inspired by the morphology of the omniphobic springtail skin[16–19] we have now introduced a reverse imprint

R. Hensel,[+] R. Helbig, Dr. H.-G. Braun, Prof. C. Werner
Max Bergmann Center of Biomaterials Dresden,
Leibniz Institute of Polymer Research Dresden
Hohe Straße 6, 01069, Dresden, Germany
E-mail: werner@ipfdd.de
A. Finn,[+] Prof. W.-J. Fischer
Technische Universität Dresden
Institute of Semiconductors and Microsystems
Nöthnitzer Straße 64, 01187, Dresden, Germany
Prof. C. Neinhuis
Technische Universität Dresden
Institute of Botany
Zellescher Weg 20b, 01217, Dresden, Germany
Prof. C. Neinhuis, Prof. C. Werner
Technische Universität Dresden
B CUBE Innovation Center for Molecular Bioengineering
Arnoldstrasse 18, 01307, Dresden, Germany
R. Hensel, A. Finn, Prof. W.-J. Fischer, Prof. C. Werner
Technische Universität Dresden,
Research Training Group "Nano- and
Biotechniques for Electronic Device Packaging",
Helmholtzstraße 18, 01069, Dresden, Germany
[+]These authors contributed equally.

lithographic technique to generate polymer membranes which combine superb wetting resistance and mechanical stability. The fabricated membranes are flexible and free-standing and, therefore, adaptable to various substrate materials and shapes for emerging applications.

Surface roughness can determine the macroscopic wetting characteristics of solid surfaces.[20] Liquids can completely wet the surface, which is referred to the Wenzel state,[21] or be sustained atop the protrusions of a rough surface with air (plastron or physical gill)[22] entrapped inside grooves underneath the liquid, which results in a heterogeneously wetted surface, known as the Cassie state.[23] The Cassie state is energetically metastable and can be transferred into the Wenzel state by increasing the pressure difference between the liquid and the entrapped air phase.[10] The related transition barrier depends on the interfacial energies of the three-phase system (liquid, solid, gas) and on the surface morphology.[24] Recently, it was found that the cross-sectional profiles of the individual surface features are crucially important for a sustained Cassie state: Overhanging profiles can prevent complete wetting by pinning the three-phase contact line even for low-surface-tension liquids, which is referred to as omniphobicity.[25,26] The skin of springtails (Collembola) provides an impressive example of such omniphobic surfaces that occurs in nature[16] and protects these skin-breathing soil arthropods against suffocation by complete wetting.[27] The entire body of springtails is covered with nanoscopic granules and interconnecting ridges, which together form a comblike pattern with cavity diameters in the range of 0.4–1 μm,[17] as exemplarily shown for the skin morphology of *Folsomia candida* in **Figure 1**a. Recent analyses demonstrated the predominant role of the nanoscopic granules of springtail skin which can prevent wetting irrespective of the surface chemistry of the structured material[18,19] and even upon immersion into many polar and nonpolar solvents.[16] Furthermore, the comblike arrangement of the surface features was found to represent a mechanically self-supporting network that allows high shear load dissipation in sand abrasion tests.[16]

Mimicking the effectively liquid-repellent and mechanically stable springtail-skin morphology in engineered materials may offer exciting opportunities for numerous emerging applications. In particular, surface features that exhibit overhanging cross-sections and are arranged in self-supporting comblike patterns may offer an unprecedented level of control over wetting phenomena. Therefore, we have used top-down manufacturing methods to develop a polymer membrane that resembles the springtail-skin morphology (Figure 1b). The omniphobic performance of the polymer membranes is demonstrated by in situ plastron collapse and long-term immersion tests. The mechanical durability of the membranes is shown by wear tests
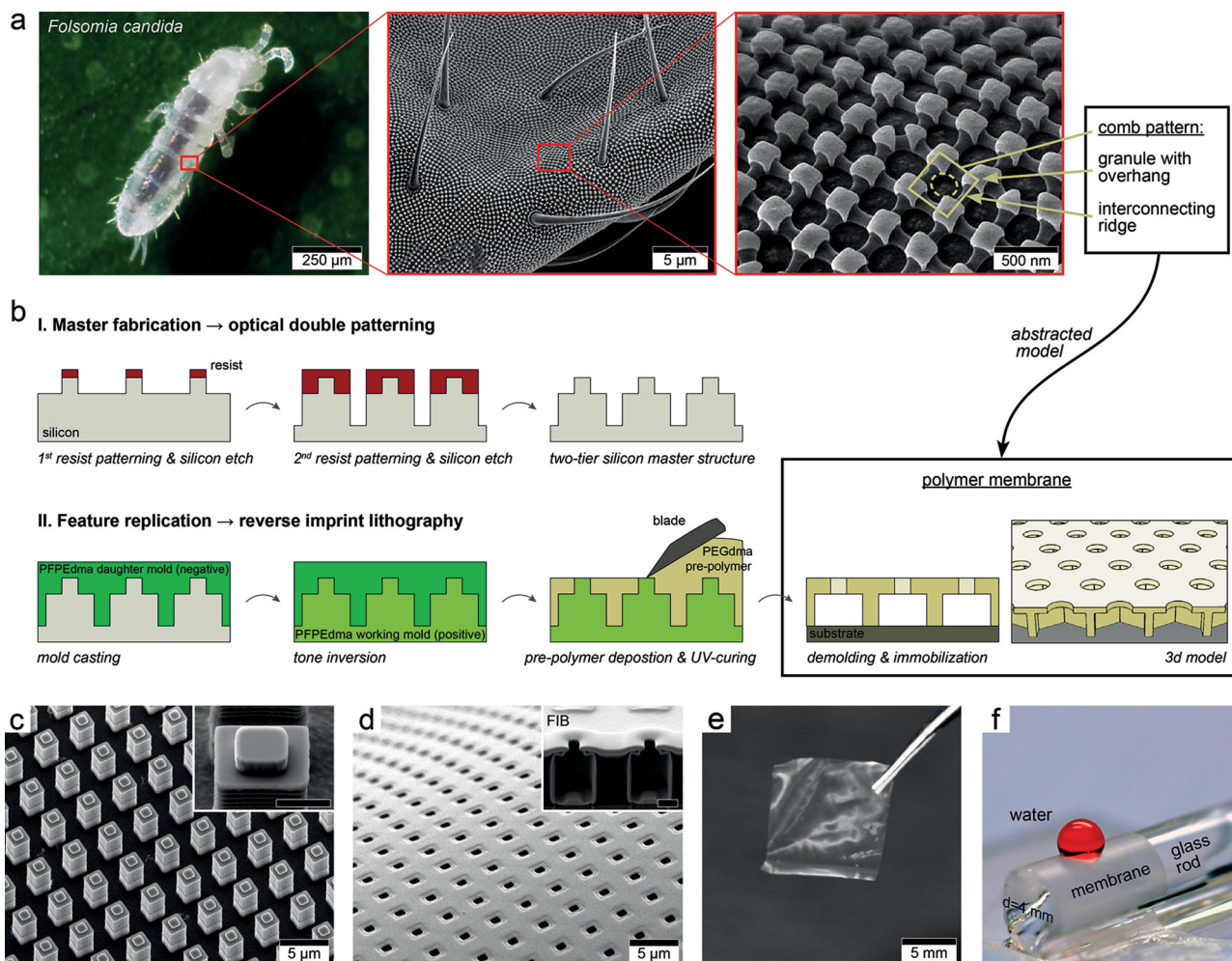
Figure 1. Springtail skin morphology and process scheme for manufacturing polymer membranes with similar structural features. a) Habitus image of *Folsomia candida*. Inserts show scanning electron micrographs (SEMs) of the characteristically contained bristles, granules, and ridges. The nanoscopic granules and interconnecting ridges form cavities, are arranged in a comblike pattern, and provide a template for the developed polymer membranes. b) Process scheme for membrane fabrication: Firstly, a two-tier silicon master structure is fabricated by optical lithography. Secondly, the master structure serves as template for reverse imprint lithography. c) SEM image of the two-tier silicon master structure (insert: detailed view of a small pillar centered on a larger pillar, scale bar: 1 μm). d) SEM image (insert: cross-section after focused ion beam preparation, scale bar: 1 μm) and e) photograph of the springtail-skin-inspired polymer membrane. f) Water droplet (colored with red dye) deposited on the membrane, which was transferred to a 4-mm diameter glass rod.

in comparison to a pillar surface by using a nanotribometer approach.

Polymer membranes were produced from a two-tier silicon master structure that serves as template for feature replication, as schematically shown in Figure 1b. Two-tier silicon master structures that consisted of small pillars centered on larger pillars were fabricated by optical overlay lithography using a mask-aligner setup with manual wafer positioning for feature dimensions larger than 3 μm or a wafer-stepper setup with automatic marker alignment for smaller features down to 500 nm. The wafer-stepper setup allowed miniaturization of the surface features due to a better overlay accuracy and higher resolution (Figure 1c). The subsequent feature replication is based on a reverse imprint lithography approach using perfluoropolyether dimethacrylate (PFPEdma) templates cast from the silicon master.[28,29] The cavities of this working mold were filled with a poly(ethylene glycol) dimethacrylate (PEGdma) prepolymer solution by doctor-blade technique without a residual layer on the small pillar structures. After subsequent cross-linking, no further post-etching steps were required to obtain a perforated membrane. Each cavity of the membrane had a narrow opening at the top, which provided an overhang inside the cavity (Figure 1d). Finally, after demolding, the flexible membrane was free-standing (Figure 1e) and, thus, transferable to various nonflat substrate materials, e.g., a glass rod (Figure 1f). With this methodology, a set of membranes with different opening diameters, $2a$, of the cavities in a square (wafer-stepper setup, $2a < 3$ μm) or hexagonal (mask-aligner setup, $2a \geq 3$ μm) lattice was fabricated.

To evaluate the wetting of membrane-coated surfaces, long-term plastron collapse tests upon complete immersion of the membranes were carried out. In addition, dynamic

Materials
Views
www.MaterialsViews.com

ADVANCED
MATERIALS
www.advmat.de

COMMUNICATION

contact angle goniometry was performed. PEGdma polymer membranes were used without any further chemical surface modification as they are intrinsically hydrophilic and lyophilic, with advancing contact angles of $\Theta_{adv,water} = 73 \pm 3°$ and $\Theta_{adv,hexadecane} = 30 \pm 3°$ of the related planar reference surfaces, respectively (Figure S1a). Membranes were placed in a liquid-flooded chamber mounted on an optical microscope for facilitating in situ observations upon hydrostatic pressure manipulation, as schematically illustrated in **Figure 2**a and described in detail previously.[18] The polymer membranes showed clearly omniphobic behavior as is obvious from the plastron formation immediately upon immersion into water or hexadecane (surface tensions $\gamma_{water} = 72.3 \times 10^{-3}$ and $\gamma_{hexadecane} = 27.5 \times 10^{-3}$ mN m^{-1}). The stability of the membrane-entrapped plastrons was followed in situ under linearly increasing hydrostatic pressure. The pressure value at which the plastron collapsed was defined as the breakthrough pressure, p_{break}. Expanding liquid fronts remained inside the narrow opening of the cavities until the three-phase contact line was depinned and the overhang was wetted (Figure 2b and Supplemental Movie M1). For both liquids, the resistance clearly depends on the opening diameter of the cavity, $2a$. For $2a < 1$ μm, the breakthrough pressure significantly increases up to values of about 3500 hPa for water and about 600 hPa for hexadecane (Figure 2d), in accordance with the previously reported pressure resistance of the springtail skin.[16,18,19] Thus we conclude that structure miniaturization allows fabrication of robust omniphobic polymer membranes. The obtained data are in line with recent studies of pillar arrays[11] and calculated values (Figure 2d) that were determined by using Equation (1):[19]

$$p_{break} = \frac{2\gamma \sin(\Theta_{adv} + \Psi)}{a} \tag{1}$$

where γ is the surface tension, Θ_{adv} is the advancing contact angle, and ψ is the maximal slope inside the cavity ($\psi = 0°$ for the membranes).

Besides enforced depinning of the triple-phase line, plastron collapse may result from liquid condensation inside the cavities or diffusion of the entrapped air into the liquid phase. Figure 2c depicts the nucleation and growth of water droplets inside the cavities. Nucleation was observed to be energetically favorable at the edges of the overhang or the bottom of the cavity.[32] Initially, condensates grew and partially merged by fusion. However, most condensates became stable and did not grow any further after approximately 2 h. This steady state persisted for more than seven days, while only a few plastrons collapsed (Supplemental Movie M2). The examined longevity of the polymer membranes is similar to that found on natural surfaces[33,34] and exceeds the values previously reported on any engineered surfaces.[35,36] Hexadecane did not condense inside the cavities due to its much lower saturation vapor pressure. Thus, the plastron was stable over time periods of at least seven days.

In sum, the springtail-skin-inspired polymer membranes are characterized by persistence against enforced wetting and long-term plastron stability in water as well as in hexadecane. Wetting transitions occurring within individual cavities did not affect adjacent cavities as the cavities are separated by impermeable walls (Supplemental Movie M1 and M2). This separation is clearly advantageous compared to commonly used pillar
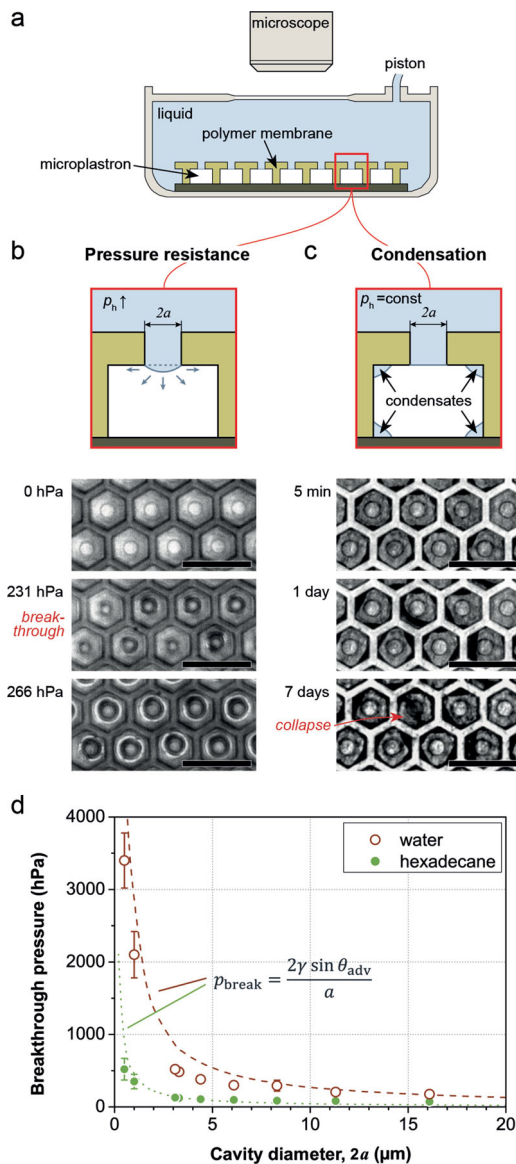

Figure 2. Immersion experiments. a) Schematic cross-sectional view of the experimental setup consisting of a liquid-flooded chamber containing the membranes, an optical microscope, and a piston for hydrostatic pressure manipulation. b) Schematic side view and optical micrograph series (top view, bright field) of the pressure-dependent collapse of the plastrons by an expanding water front inside the cavities (scale bars: 50 μm). c) Schematic side view and optical micrograph series (top view, bright field) representing the time-dependent partial filling of the membrane cavities by condensation (scale bars: 50 μm). d) Breakthrough pressures at polymer membranes with varying opening diameters, demonstrating the robustness of the Cassie state for water (brown circles) and hexadecane (green dots). Circles and dots represent the experimental data, lines the calculated values; see Equation (1).

structures, where locally initialized wetting is often followed by immediate sideways propagation of the fluid front.[37] The overhanging cross-sections of the membrane cavities allow omniphobicity, i.e., resistance even against wetting of low-surface-tension liquids, without any surface modification. In fact, the hydrophilic characteristics of the polymer membrane

COMMUNICATION

results in an enhanced adhesion of the liquid–solid interface in comparison to low energy surfaces:[33] The interface sticks to the membrane and the loss of the plastron due to vibrations or turbulent flow can be avoided (Salvinia effect).[33]

In addition to the immersion tests, the polymer membranes were further characterized by using dynamic contact angle goniometry (Figure S1). For both liquids, the obtained advancing contact angles at the polymer membranes were higher than the intrinsic one, which indicates the Cassie state of the applied liquids (Figure S1a). The advancing contact angles increased with larger opening diameters due to the reduced fraction of the projected solid–liquid contact area, f_s, which simultaneously enhanced the fraction of the liquid–air interface $(1 - f_s)$. The arrangement of the array of cavities inside the membranes was kept constant for the contact-angle measurements and, therefore, the projected wetted solid area ranges between 0.75 and 0.98 depending on the cavity diameter. The apparent contact angle varies only slightly in comparison to the intrinsic contact angles due to the high solid area fractions, which is in line with the model of Cassie and Baxter; Equation (2):[30]

$$\cos \theta_{app} = r_f \, f_s \cos \theta_Y + f_s - 1 \qquad (2)$$

where r_f is the roughness ratio of the wetted solid area. The liquids could penetrate inside the narrow cavity openings due to the hydrophilic and lyophilic nature of the polymer membrane. As a consequence, the contact line is pinned by the formation of capillary bridges (Figure S1b) in accordance with the model of Dufour et al.[31] The adhesive characteristic of the membrane is further reproduced by the receding contact angle data, which decreases with larger opening diameters due to more pronounced capillary bridges.

To evaluate the mechanical durability of the polymer membranes, wear tests were performed in comparison to pillar structures commonly used for mimicking superhydrophobic surfaces.[3] PEGdma polymer was used for both the membranes and the pillar arrays to ensure comparability of the intrinsic mechanical properties. Furthermore, the height of the surface features and the lattice parameter of the tested arrays were adjusted to be similar. Shear forces were applied by an oscillating steel ball in combination with a load (**Figure 3**). Load dissipation and failure mode of surface structures clearly differed between the membranes, which were plastically deformed and delaminated from the substrate, and the pillar array, which broke at the bottom where the highest bending stress occurred. The membranes provided a continuous, self-supporting surface that resisted loads of 200 to 500 mN depending on the comb wall width (Figure 3a). In contrast, the mechanical stability of the pillar structures was much lower and ranged from 1 to 75 mN depending on the pillar diameter (Figure 3b). Thus, membrane-coated surfaces showed a significantly higher mechanical stability than did surfaces covered with pillar arrays.

A novel and promising strategy for the fabrication of omniphobic polymer coatings was introduced. Mechanical durability and pronounced, long-term resistance against wetting upon complete immersion, the most striking features of the springtail skin, were effectively reproduced in polymer membranes that mimic the contained comblike patterned cavities with overhangs. Miniaturization of the surface features was found to allow a particularly high pressure resistance. Omniphobicity of
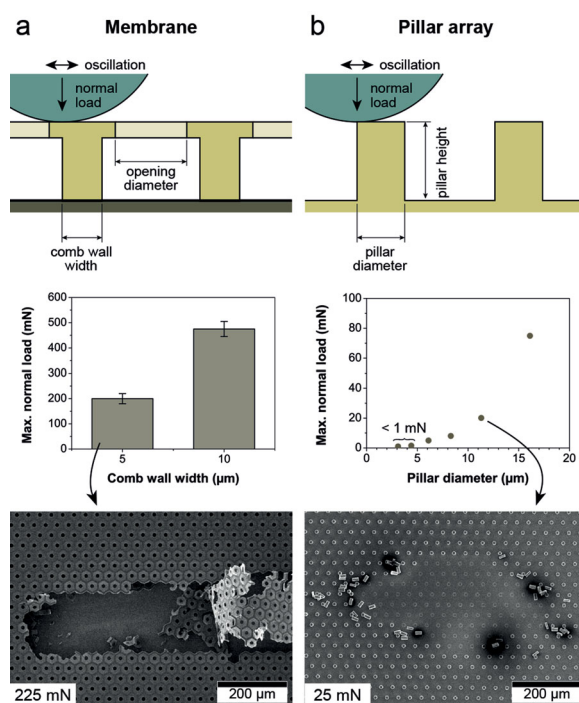

Figure 3. Wear tests of a) polymer membranes in comparison to b) pillar arrays: Schematic representation of the experimental setup consisting of an oscillating steel ball, pressed onto the structured surfaces. Experimental data of maximal normal loads the surfaces can resist without destruction and SEM images after failure.

the produced polymer membranes was solely achieved through control over structural features, namely, the presence of overhanging cross-sections of the membrane cavities, independent of the surface chemistry. The produced membranes can be precisely adjusted with respect to morphological and compositional characteristics, and applied to various different, even nonflat bulk materials. Accordingly, a broad spectrum of emerging applications may benefit, particularly when the membranes are utilized under conditions of complete immersion, including examples as different as liquid handling in microfluidics and biofouling prevention on ship hulls and pipes. Upscaling of the utilized reverse imprint lithography technique may be achieved by adaptation of roll-to-roll processing schemes.[28]

Experimental Section

Details of the materials and experimental methods used are available in the Supporting Information.

Supporting Information

Supporting Information is available from the Wiley Online Library or from the author.

Acknowledgments

ADVANCED
MATERIALS

COMMUNICATION

[1] C. Neinhuis, W. Barthlott, *Ann. Bot.* **1997**, *79*, 667.
[2] W. Barthlott, C. Neinhuis, *Planta* **1997**, *202*, 1.
[3] D. Quéré, M. Reyssat, *Phil. Trans. R. Soc. A* **2008**, *366*, 1539.
[4] A. Solga, Z. Cerman, B. F. Striffler, M. Spaeth, W. Barthlott, *Bioinspir. Biomim.* **2007**, *2*, S126.
[5] C.-H. Choi, U. Ulmanella, J. Kim, C.-M. Ho, C.-J. Kim, *Phys. Fluids* **2006**, *18*, 087105.
[6] V. Eyring, H. Köhler, A. Lauer, B. Lemper, *J. Geophys. Res.* **2005**, *110*, 2156.
[7] C. M. Kirschner, A. B. Brennan, *Annu. Rev. Mater. Res.* **2012**, *42*, 211.
[8] J. Hasan, R. J. Crawford, E. P. Ivanova, *Trends Biotechnol.* **2013**, *31*, 295.
[9] K. Koch, B. Bhushan, W. Barthlott, *Prog. Mater. Sci.* **2009**, *54*, 2137.
[10] Q. S. Zheng, Y. Yu, Z. H. Zhao, *Langmuir* **2005**, *21*, 12207.
[11] H. Zhao, K.-C. Park, K.-Y. Law, *Langmuir* **2012**, *28*, 14925.
[12] T. Verho, C. Bower, P. Andrew, S. Franssila, O. Ikkala, R. H. Ras, *Adv. Mater.* **2011**, *23*, 673.
[13] E. Huovinen, J. Hirvi, M. Suvanto, T. A. Pakkanen, *Langmuir* **2012**, *28*, 14747.
[14] B. Pokroy, S. H. Kang, L. Mahadevan, J. Aizenberg, *Science* **2009**, *323*, 237.
[15] A. Finn, B. Lu, R. Kirchner, X. Thrun, K. Richter, W.-J. Fischer, *Microelectron. Eng.* **2013**, *99*, 112.
[16] R. Helbig, J. Nickerl, C. Neinhuis, C. Werner, *PloS One* **2011**, *6*, e25105.
[17] J. Nickerl, R. Helbig, H.-J. Schulz, C. Werner, C. Neinhuis, *Zoomorphology* **2013**, *132*, 183.
[18] R. Hensel, R. Helbig, S. Aland, A. Voigt, C. Neinhuis, C. Werner, *NPG Asia Mater.* **2013**, *5*, e37.
[19] R. Hensel, R. Helbig, S. Aland, H.-G. Braun, A. Voigt, C. Neinhuis, C. Werner, *Langmuir* **2013**, *29*, 1100.
[20] D. Quéré, *Annu. Rev. Mater. Res.* **2008**, *38*, 71.
[21] R. Wenzel, *Ind. Eng. Chem.* **1936**, *28*, 988.
[22] O. Pedersen, T. D. Colmer, *J. Exp. Biol.* **2012**, *215*, 705.
[23] A. Cassie, S. Baxter, *Trans. Faraday Soc.* **1944**, *40*, 546.
[24] L. Barbieri, E. Wagner, P. Hoffmann, *Langmuir* **2007**, *23*, 1723.
[25] A. Tuteja, W. Choi, M. L. Ma, J. M. Mabry, S. A. Mazzella, G. C. Rutledge, G. H. McKinley, R. E. Cohen, *Science* **2007**, *318*, 1618.
[26] A. Marmur, *Langmuir* **2008**, *24*, 7573.
[27] J. Noble-Nesbitt, *J. Exp. Biol.* **1963**, *40*, 681.
[28] J. P. Rolland, B. W. Maynor, L. E. Euliss, A. E. Exner, G. M. Denison, J. M. DeSimone, *J. Am. Chem. Soc.* **2005**, *127*, 10096.
[29] R. Hensel, H.-G. Braun, *Soft Matter* **2012**, *8*, 5293.
[30] A. Marmur, *Langmuir* **2003**, *19*, 8343.
[31] R. Dufour, M. Harnois, V. Thomy, R. Boukherroub, V. Senez, *Soft Matter* **2011**, *7*, 19 9380.
[32] S. Herminghaus, M. Brinkmann, R. Seemann, *Annu. Rev. Mater. Res.* **2008**, *38*, 101.
[33] W. Barthlott, T. Schimmel, S. Wiersch, K. Koch, M. Brede, M. Barczewski, S. Walheim, A. Weis, A. Kaltenmaier, A. Leder, H. F. Bohn, *Adv. Mater.* **2010**, *22*, 2325.
[34] A. Balmert, H. Florian Bohn, P. Ditsche-Kuru, W. Barthlott, *J. Morphol.* **2011**, *272*, 442.
[35] M. S. Bobji, S. V. Kumar, A. Asthana, R. N. Govardhan, *Langmuir* **2009**, *25*, 12120.
[36] R. Poetes, K. Holtzmann, K. Franze, U. Steiner, *Phys. Rev. Lett.* **2010**, *105*, 166104.
[37] B. Mognetti, J. Yeomans, *Phys. Rev. E* **2009**, *80*, 056309.